Eur. Phys. J. B **57**, 229–234 (2007)
DOI: 10.1140/epjb/e2007-00176-5

THE EUROPEAN PHYSICAL JOURNAL B

From compact point defects to extended structures in silicon

Y.A. Du[1,a], R.G. Hennig[2,3], T.J. Lenosky[4], and J.W. Wilkins[3]

[1] Department of Physics, Wake Forest University, Winston-Salem, North Carolina 27109, USA
[2] Department of Materials Science and Engineering, Cornell University, Ithaca, New York 14853, USA
[3] Department of Physics, Ohio State University, Columbus, Ohio 43210, USA
[4] Department of Materials Science and Engineering, Ohio State University, Columbus, Ohio 43210, USA

Received 5 October 2006 / Received in final form 16 March 2007
Published online 22 June 2007 –

Abstract. First-principles studies of the formation and dynamics of silicon interstitial-clusters suggest a possible growth mechanism of silicon interstitial-chains as seen in macroscopic {311} planar defects. The relative populations of the three lowest-energy silicon tri-interstitials equilibrate within a few microseconds. Unfortunately, the tri-interstitial chain is unstable, quickly decaying to the ground-state interstitial. However, the four-interstitial chain with escape barriers of 0.54 eV is relatively stable and can be formed by exothermic capture of an interstitial by the ground-state tri-interstitial. This first successful step seems capable of growing longer chains. If one chain eases the formation of a second parallel chain, this may start the process of forming {311} planar defects.

PACS. 61.72.Cc Kinetics of defect formation and annealing – 61.72.Ji Point defects (vacancies, interstitials) and defect clusters – 71.15.Mb Density functional theory, local density approximation, gradient and other corrections – 71.15.Pd Molecular dynamics calculations

1 Introduction

Ion implantation into silicon introduces a large number of excess interstitial atoms, which can condense during the subsequent annealing step to form macroscopic {311} planar defects [1–4]. The annealing process is required to remove the lattice damage. Small interstitial defects are invisible to transmission electron microscope (TEM) studies [5] while the larger {311} defect has been observed in TEM after 15 s annealing at 1100 K [6]. During annealing, the boron dopant atoms show enhanced diffusion, leading to an undesirable spreading of the dopant spatial profiles [6,7]. This enhanced boron diffusion is believed to be caused by interactions with interstitial atoms released from the {311} defects [6].

The structure of the {311} planar defect consists of a set of parallel ⟨110⟩-chains sitting side by side on the {311} plane [2–4], as shown in Figure 1. The interstitial ⟨110⟩-chain is a linear defect structure of silicon interstitial-atoms aligned in the ⟨110⟩ direction. For small numbers of interstitial atoms, compact defect geometries are favored [8–12], but ⟨110⟩-chain structures become energetically favorable as more interstitials are added [4,11].

Viewing the {311} planar defect as a set of parallel chains perpendicular to the plane of Figure 1 suggests hunting for the mechanisms of growing such chains. In order to understand the formation of a single ⟨110⟩-chain, one very important step appears to be how compact clusters of several interstitial atoms grow into short chain structures. In this work, we use the nudged elastic band (NEB) [13,14] and dimer methods [15] within density functional theory (DFT) as well as a tight-binding [16] (TB) model to study the transition from compact defect structures to short interstitial chains. We show that under typical annealing conditions (1) the three lowest-energy tri-interstitials I_3 reach thermal equilibrium within a few microseconds, (2) the I_3-chain is unstable because it lies

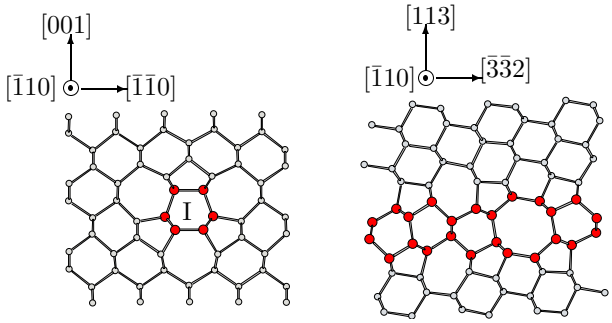

Fig. 1. Extended silicon interstitial defects. As shown in (a), the ⟨110⟩ interstitial chain denoted by I is a linear defect structure elongated along the ⟨110⟩ direction. The {311} planar defect shown in (b) consists of parallel ⟨110⟩ chains lying side by side on the {311} plane.

[a] e-mail: dyj@pacific.mps.ohio-state.edu

in a shallow local minimum, (3) the I_4-chain, lying in a deeper local minimum, can form from the ground-state tri-interstitial I_3^a by capturing a single interstitial in an exothermic reaction, and (4) to go from an I_4-chain to a ground state I_4^a requires a 0.54 eV activation energy.

Interstitial clusters containing less than five interstitials prefer a compact over a chain structure [8–12]. For instance, the formation energy of the compact tri-interstitial is 1 eV lower than that of the I_3-chain, and the formation energy of the compact four-interstitial is 1.5 eV lower than that of the I_4-chain. The compact ground-state four-interstitial I_4^a is an extremely stable [10,17] and immobile structure [17,18]. Birner et al. showed that the core structure of the I_4^a remains intact in the presence of an additional attached interstitial atom in the molecular dynamics (MD) simulations [17]. If an I_4-chain captures extra interstitials before decaying to an I_4^a, the system can develop an extended chain structure that is the building block of {311} planar defects [2–4]. On the other hand, if a system falls into the ground state I_4^a, the growth process of chain structures is frustrated.

2 Method

The density functional calculations are performed with the Vienna Ab-initio Simulation Package (VASP) [19,20] employing the Perdew-Wang generalized gradient approximation (GGA) [21] and ultra-soft Vanderbilt-type pseudopotentials [22] as provided by Kresse and Hafner [23]. A plane-wave kinetic energy cut-off of 250 eV and a $3\times3\times3$ k-mesh for the 64-atom cells ensure the energy convergence of the defect formation to 10 meV. An increased cutoff energy of 300 eV and a larger $4\times4\times4$ k-point mesh change the formation energy of the compact tri-interstitial I_3^b by less than 3 meV and the relaxed atomic positions by less than 0.005 Å.

The pathways connecting the three lowest-energy tri-interstitial structures are obtained from the MD simulations [24] and refined using the climbing-image NEB (CI-NEB) [14] method within DFT. The CI-NEB method computes the transition path connecting the three lowest-energy tri-interstitials using a 64-atom $(2\times2\times2)$ cubic supercell of silicon with a lattice constant of 5.432 Å. When minima along the path are found during the NEB relaxation, the path is further refined by relaxing the new minima to obtain local minima. The NEB re-runs using each adjacent local minima as end points. Thus, for the final NEB calculation, there is only one saddle point between each pair of adjacent local minima along the path. Each image is relaxed until the perpendicular force is less than 20 meV/Å. Moreover, the CI-NEB method guarantees that each saddle point is accurately determined [14]. Figure 2 shows the resulting transition path connecting the three lowest-energy tri-interstitial defects.

Harmonic transition state theory [25] determines the transition rate Γ between any two adjacent minima along the path connecting I_3^b to I_3^a by

$$\Gamma = \Gamma_0 e^{-\Delta E/k_B T}, \tag{1}$$

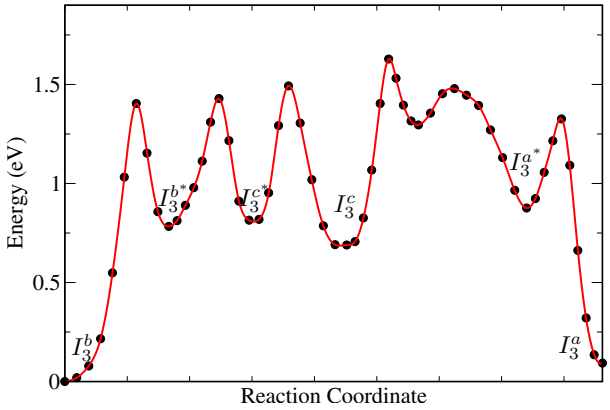

Fig. 2. Transition path connecting I_3^b, I_3^c, and I_3^a in DFT-GGA. $I_3^{b^*}$, $I_3^{c^*}$, and $I_3^{a^*}$ are intermediate structures along the transition path. The energy path is computed within $64+3$ atom supercell. I_3^a is the real ground-state tri-interstitial in a larger cell (see Tab. 1).

where ΔE denotes the activation energy and Γ_0 is the prefactor of diffusion. The CI-NEB ensures that the image with the highest energy is at the saddle point and also provides the activation energy. On the other hand, the prefactor Γ_0 is given by:

$$\Gamma_0 = \prod_i^{3N-3} \nu_i^{min} / \prod_i^{3N-4} \nu_i^{sad}, \tag{2}$$

where ν_i^{min} and ν_i^{sad} are the phonon frequencies at the minimum and saddle point, respectively, calculated by the dynamical matrix method. Each atom is displaced in the $\hat{x}$, $\hat{y}$, and $\hat{z}$ directions by 0.03 Å and the calculated forces are used to construct the Hessian of the system, whose eigenvalues are proportional to the square of phonon frequencies.

Dimer searches [15] using the tight-binding model by Lenosky et al. [16] study the landscape surrounding an I_4-chain, in order to reveal the formation processes and stability of the structure. In the dimer search, we choose a dimer separation of $2\Delta R = 10^{-2}$ Å and finite difference steps for rotation and translation of $d\theta = 5\times10^{-3}$ and $dR = 5\times10^{-3}$ Å, respectively. The maximum move is 0.5 Å. The stopping criterion is that the force on the dimer center be less than 10 meV/Å. These parameters are detailed in reference [15]. The dimer searches use the Γ point sampling of the TB model and a $216+4$ supercell. The dimer searches find saddle points surrounding the I_4-chain that we then relax to the neighboring local minima. Finally, VASP-DFT relaxes the neighboring minima.

The nudged elastic band method within DFT computes the transition path for the saddle point discovered by the dimer method, leading to the formation of the I_4-chain from the ground state I_3^a using a $216+4$ atom supercell, a 250 eV cut-off energy, and a $2\times2\times2$ k-mesh. The NEB with the same parameters also computes the transition path between the two constructed end-points of an I_4-chain and a ground state I_4^a. Each of the images

Table 1. Formation energies for all the minima along the transition path shown in Figure 2 connecting I_3^b, I_3^c, and I_3^a within $64+3$ and $216+3$ atom supercells, respectively. E_f^{64} and E_f^{216} denote the formation energy in $64+3$ and $216+3$ atom supercells, respectively. Change in energies going to larger cells estimates the finite size error. The energies of the $64+3$ atom supercell are accurate to 0.6 eV or 0.2 eV per defect atom.

Structure	E_f^{64} (eV)	E_f^{216} (eV)
I_3^b	7.356	7.104
$I_3^{b^*}$	8.139	7.670
$I_3^{c^*}$	8.169	7.730
I_3^c	8.046	7.401
$I_3^{a^*}$	8.232	7.790
I_3^a	7.449	6.723

along the paths is relaxed until the perpendicular force is less than 30 meV/Å.

3 Transition path connecting the three lowest-energy tri-interstitials

From analysis of tight-binding molecular dynamics trajectories, Richie et al. identified the three lowest-energy tri-interstitials I_3^a, I_3^b, and I_3^c [24]. During the MD simulations, the mobile I_3^b [26] interstitial first transformed into the I_3^c structure (0.3 eV higher in energy) before transforming into the ground state I_3^a structure (0.4 eV lower in energy).

Figure 2 shows the relaxed transition pathway from the CI-NEB calculations connecting the three lowest-energy tri-interstitials I_3^b, I_3^c, and I_3^a within DFT, showing that an I_3^a can be developed from an I_3^b. The three intermediate structures along the path are denoted by $I_3^{b^*}$, $I_3^{c^*}$, and $I_3^{a^*}$. Table 1 shows the energies of all six local minima. Note that, although I_3^b is the ground state in $64+3$ atom cells (as shown in Fig. 2), in larger $216+3$ atom cells I_3^a holds that distinction. Moreover, Richie et al. confirmed that this relative ordering holds even in $512+3$ atom cells [24]. Table 2 summarizes the prefactors and energy barriers for all transitions along the path, both the forward and reverse directions. Notably, the transition $I_3^b \rightarrow I_3^{b^*}$ has the highest barrier and the second lowest prefactor among all other transitions along the path. Thus, it is the dominant step for a system to go from I_3^b to I_3^a at typical annealing temperatures (∼1100 K). Using the rate limiting step ($I_3^b \rightarrow I_3^{b^*}$), we estimate the transition rate from the compact I_3^b structure to the ground state I_3^a to be $1/\tau = 7.8$ THz $\exp(-1.4\ \mathrm{eV}/k_BT)$.

The transition rates among the three tri-interstitial structures estimate the equilibration time of their relative populations during thermal annealing conditions. At typical annealing temperatures of 1100 K, the transition rate from I_3^b to I_3^a is around 2.5×10^6 Hz. This indicates that the relative populations of all three tri-interstitial defects, I_3^a, I_3^b, and I_3^c reach thermal equilibrium within a few microseconds. This equilibration time is many orders of magnitude shorter than the 15 s which is required for the observation of {311} planar defects after thermal annealing at the same temperature of 815 °C [6]. This vast difference between time scales indicates that a ground state I_3^a forms long before {311} planar defects and may serve as a nucleating center for the extended structures [24]. Also, since an I_2^a can capture a single interstitial to develop an I_3^b [27], a ground state I_3^a may form through the reaction $I_2^a + I \rightarrow I_3^b \rightarrow I_3^a$.

Table 2. Transition rates between two adjacent minima along the transition path from I_3^b to I_3^a within $64+3$ atom supercells. The NEB [13] method and harmonic transition state theory [25] calculate the energy barriers and prefactors, respectively. The transition $I_3^b \rightarrow I_3^{b^*}$ is the dominant mechanism for a system to go from I_3^b to I_3^a.

Transition	Prefactor (THz)		Barrier (eV)	
	forward	backward	forward	backward
$I_3^b \longrightarrow I_3^{b^*}$	7.8	540	1.4	0.62
$I_3^{b^*} \longrightarrow I_3^{c^*}$	240	180	0.65	0.61
$I_3^{c^*} \longrightarrow I_3^c$	14	170	0.68	0.80
$I_3^c \longrightarrow I_3^{a^*}$	260	13	0.94	0.75
$I_3^{a^*} \longrightarrow I_3^a$	3.6	480	0.45	1.2

[a] We ignore the shallow minimum between I_3^c and $I_3^{a^*}$.

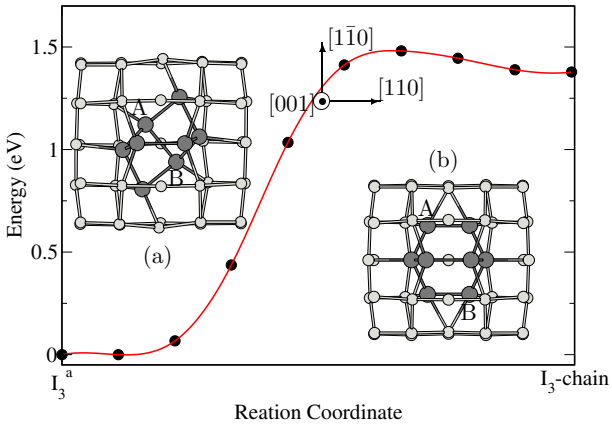

Fig. 3. Transition path connecting an I_3^a and an I_3-chain in DFT-GGA. The structures of the I_3^a and the I_3-chain viewed from [001] are shown in (a) and (b), respectively. It indicates that a chain structure cannot be developed from an I_3^a directly, since the shallow barrier of 0.1 eV from an I_3-chain to an I_3^a makes the I_3-chain unstable at typical annealing temperatures.

4 Development of interstitial chains

Figure 3 shows that the direct formation of an I_3-chain from a ground-state tri-interstitial I_3^a is energetically unfavorable. Insets (a) and (b) show the ground state I_3^a and the I_3-chain, respectively, viewed from the [001] direction. A 1.2 Å displacement of atoms A and B, respectively, as described in reference [24], relates the two structures. The formation energy of the I_3-chain is 1.4 eV higher than that of the I_3^a. The NEB method within a $64+3$ atom

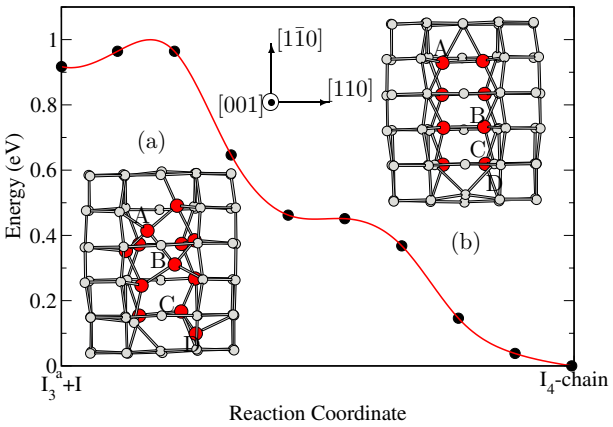

Fig. 4. Transition path between the I_3^a combined with a single interstitial and the I_4-chain in DFT-GGA. The structure of the bound state of an I_3^a and a single interstitial, which is identified by dimer searches, is shown in (a), while the structure of the I_4-chain is shown in (b). It indicates that a chain structure can be developed from an I_3^a combined with a single interstitial, since the energy drops about 0.92 eV from the bound state of an I_3^a and a single interstitial to the I_4-chain with a tiny barrier of 80 meV.

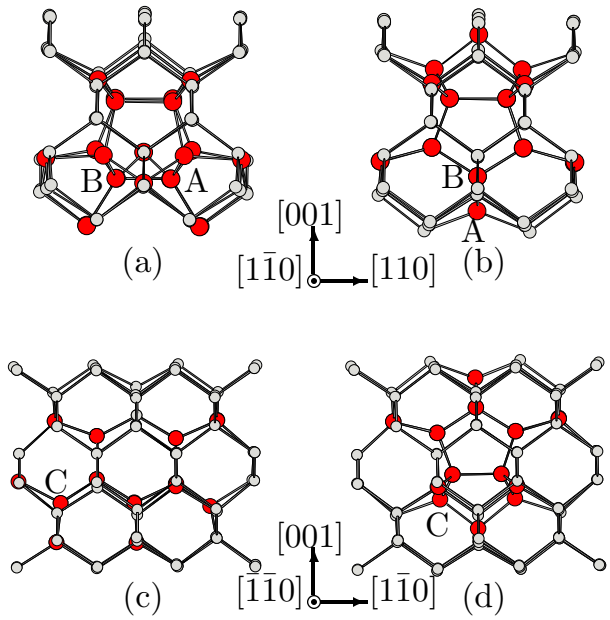

Fig. 5. The structure of the I_4-chain and the compact ground state I_4^a. An I_4-chain is a short ⟨110⟩-chain (see Fig. 4), and an I_4^a is a "squeezed" I_4-chain with all atoms fully bonded [8]. The I_4-chain viewed from the [1$\bar{1}$0] and [110] directions are shown in (a) and (c), respectively. The ground state I_4^a viewed from the [1$\bar{1}$0] and [110] directions are shown in (b) and (d), respectively. Atoms A, B and C are the three most displaced atoms during the transition between the I_4-chain and the ground state I_4^a.

supercell determines the energy barrier of the transition. The energy barrier for a system to go from an I_3^a to an I_3-chain is 1.5 eV. The transition from an I_3-chain to an I_3^a has a small energy barrier of 0.1 eV, showing that the I_3-chain is unstable at typical annealing temperatures. The formation of an I_3-chain from an I_3^a requires 1.4 eV, hence the I_3-chain structure is not present in any significant amounts at typical annealing temperatures.

We show that the I_4-chain is metastable at annealing temperatures and might be the first step in the formation of extended interstitial chains. The formation energy of the I_4-chain (2.46 eV/atom) on a per-atom basis is lower than the I_3-chain (2.70 eV/atom), suggesting that the I_4-chain may lack the instability that we have found for the I_3-chain. To confirm the stability and formation process of the I_4-chain, we apply the dimer-search scheme to explore the neighboring local saddle points and corresponding minima of the I_4-chain. Nearly two hundred TB dimer searches find sixteen [28] saddle points and neighboring local minima. Twelve of these sixteen TB minima are stable in DFT relaxations and do not relax back to the I_4-chain. Inset (a) of Figure 4 shows that one of these eleven minima, corresponding to a ground-state tri-interstitial I_3^a combined with a single interstitial, has a low formation energy of 0.92 eV [29] above the I_4-chain in DFT. As illustrated in Figure 4, the NEB method within DFT calculates an accurate transition path between the I_3^a combined with a single interstitial and the original I_4-chain. The I_4-chain forms easily by an I_3^a (which we have shown to be a distorted I_3-chain in the inset (a) of Fig. 3) reacting with a single interstitial found by dimer searches. Inset (a) shows the local minimum is an I_3^a combined with a single interstitial when viewed along the ⟨001⟩ direction. The single-interstitial dumbbell is denoted by atoms C and D. Inset (b) shows the I_4-chain viewed from the ⟨001⟩ direction. Atoms A and B are the same as atoms A and B described in Figure 3. As shown in Figure 4, the energy drops 0.92 eV from the bound state of an I_3^a and a single interstitial to the I_4-chain with a small energy barrier of 80 meV. Hence, the reaction of an I_3^a with a single interstitial can easily lead to the formation of the I_4-chain. Figures 2 and 4 reveal such a microscopic process that a system transforms from a compact structure to an extended chain-like structure. It might be the first step in the formation of extended interstitial chains.

5 Formation of the ground-state four-interstitial

The nudged elastic band method calculates the transition path between the two constructed end-points: the I_4-chain (see Figs. 5a and 5c) and the compact I_4^a (see Figs. 5b and 5d), suggesting the I_4^a can form from the I_4-chain. We construct two such end points with the biggest atomic displacements smaller than bond length of 2.35 Å. The largest atomic displacement between the two end points is 2.2 Å as demonstrated by atom B in Figures 5a and 5b. The total displacement between these two endpoints is 4.34 Å in the $220 \times 3 - 3$ dimensional space corresponding to a 216+4 atom supercell. Four atoms have large displacements (>1.2 Å) during the transition while all other atoms have a displacement less than 1.0 Å. This suggests that

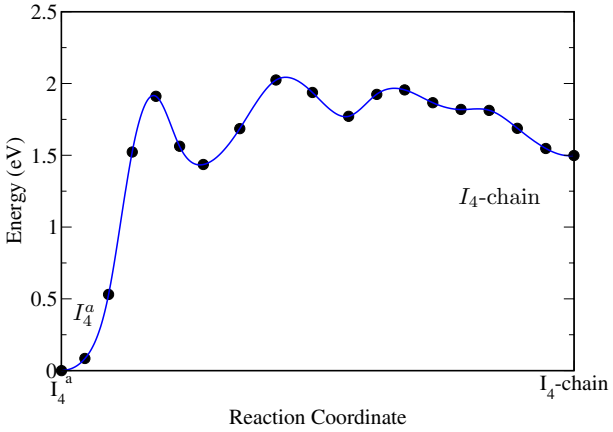

Fig. 6. Transition path connecting a ground state I_4^a and an I_4-chain calculated by relaxing initially linear-interpolated path between the two end points (see Fig. 5). The NEB method in DFT with a 250 eV cut-off energy and a $2 \times 2 \times 2$ k-mesh calculates the transition path. This pathway requires a 0.54 eV barrier for a system to transform from an I_4-chain to an I_4^a.

the transition path determined by these two end points, shown in Figure 5, might have a low transition barrier.

Figure 6 shows the calculated transition path connecting the I_4-chain and the ground state I_4^a, indicating that the energy barrier for a system to go from the I_4-chain to the ground state I_4^a is 0.54 eV. On the other hand, the reverse process requires an activation energy of 2.0 eV. This confirms that an I_4^a is a stable structure from which it is hard for a system to escape.

6 Discussion

Figure 4 suggests the exothermic reaction $I_3^a + I \rightarrow I_4$-chain might be the first step for the formation of interstitial chains. It shows a migrating single interstitial can be absorbed by an I_3^a without any additional energy barrier. The total formation energy of an isolated I_3^a and a single interstitial is 0.3 eV below the saddle point between the I_4-chain and the I_3^a combined with a single interstitial. On the other hand, the diffusion barrier for a single interstitial is also 0.3 eV [26,30,31]. Hence, it does not cost any additional energy for a migrating single interstitial to approach a ground-state tri-interstitial I_3^a and combine into an I_4-chain. This allows interstitial defects to grow into a short $\langle 110 \rangle$ chain structure without being trapped in the stable I_3^a. Moreover, the total formation energy of an isolated I_4-chain and a single interstitial is 1.8 eV above an I_5-chain, which suggests that the I_5-chain can be formed by a strongly exothermic reaction between an I_4-chain and a single interstitial. In the large number limit of n, the formation energy of an I_n-chain is 1.7 eV per atom [4]. Since the formation energy of a single interstitial is 3.8 eV, the formation energy of an isolated I_n-chain and a single interstitial is 2.1 eV above an I_{n+1}-chain in the large number limit of n. Hence, the trend that an I_{n+1}-chain ($n \geq 3$) can be developed from an isolated I_n-chain and a single interstitial by a strongly exothermic reaction persists from a short to long chain [32]. This implies that a short chain, such as an I_4-chain, can keep growing into a longer chain under the presence of a large excess of interstitials during ion implantation [6] or electron irradiation [1]. If one chain facilitates the formation of a second parallel chain, this might start the process of forming {311} planar defects. The growth of the $\langle 110 \rangle$ chain and {311} planar defects is accompanied by a reduction in strain energy; hence, it is expected that the kinetics of the defect growth are controlled by the long-range strain field induced by the defects [33].

The nudged elastic band method shows that the barrier for a system to transform from the I_4-chain to the ground state I_4^a is 0.54 eV [34]. This reveals a possible growth mechanism for the ground state I_4^a, namely $I_3^a + I \rightarrow I_4$-chain $\rightarrow I_4^a$. However, the 0.54 eV barrier is an upper bound for this transition. A lower barrier may exist, but it is difficult with the current method to carry out an even more exhaustive search [35]. We are planning to investigate the energy landscape of four interstitials more carefully in subsequent work.

Silicon extended structures can form in various ways. *First*, $I_3^a + I + I \rightarrow I_4$-chain $+ I \rightarrow I_5$-chain, an I_4-chain with an escape barrier of 0.54 eV can capture a single interstitial to develop an I_5-chain before decaying to a ground state I_4^a. *Second*, $I_3^a + I_2^a \rightarrow I_5$-chain or $I_3^a + I_3^b \rightarrow I_6$-chain, a ground-state tri-interstitial I_3^a can directly capture a mobile ground-state di-interstitial I_2^a [27,36] or a mobile tri-interstitial I_3^b [26] to develop an I_5- or I_6-chain, respectively, which can grow into longer chains by capturing of interstitials. These two approaches mentioned above provide the mechanism for a system to avoid the ground state I_4^a in developing a longer chain which is energetically favorable. *Third*, $I_3^a + I \rightarrow I_4$-chain $\rightarrow I_4^a$, the I_4-chain does decay to an I_4^a so that the growth of an interstitial chain is frustrated. The immobile I_4^a may keep capturing various interstitials to grow into a large conglomerate, which might, eventually, transform into certain extended structures. We emphasize that, in any case mentioned above, the ground-state tri-interstitial serves as a nucleating center for the extended defect structures in silicon.

7 Conclusion

Tight-binding and density-functional calculations use the dimer-search and nudged elastic band method as well as harmonic transition state theory to determine how $\langle 110 \rangle$ interstitial chains form from compact tri-interstitial defects in silicon. The three lowest-energy tri-interstitial defects reach thermal equilibrium within a few microseconds at typical annealing temperatures. It is energetically unfavorable for the ground-state tri-interstitial to transform directly into a chain structure. Instead, it can form a four-interstitial chain by capturing a migrating single interstitial without any additional energy. The I_4-chain is suspected of being a starting structure for the growth of an

interstitial chain. In addition, we reveal a possible formation mechanism of the ground-state four-atom interstitial from an I_4-chain. The upper limit of the energy barrier for a system to go from an I_4-chain to a ground state I_4^a is 0.54 eV. Finally, we illustrate that the silicon ground-state tri-interstitial serves as a possible nucleating center for the extended defect structures in silicon.

We thank Stephen A. Barr, Kaden R.A. Hazzard, Jeongnim Kim, and William Parker for valuable discussion. The work was supported in part by DOE-Basic Energy Sciences, Division of Materials Sciences (DE-FG02-99ER45795) and by National Science Foundation, CISE (GRT961718/745316). Computing resources were provided by the Ohio Supercomputing Center.

References

1. I.G. Salisbury, M.H. Loretto, Philos. Mag. A **39**, 317 (1979)
2. S. Takeda, Jpn J. Appl. Phys. **30**, L639 (1991)
3. M. Kohyama, S. Takeda, Phys. Rev. B **46**, 12305 (1992)
4. J. Kim, J.W. Wilkins, F.S. Khan, A. Canning, Phys. Rev. B **55**, 16186 (1997)
5. J.L. Benton, S. Libertino, P. Krighøj, D.J. Eaglesham, J.M. Poate, S. Coffa, J. Appl. Phys. **82**, 120 (1997)
6. D.J. Eaglesham, P.A. Stolk, H.J. Grossmann, J.M. Poate, Appl. Phys. Lett. **65**, 2305 (1994)
7. P.A. Stolk, H.J. Gossmann, D.J. Eaglesham, D.C. Jacobson, C.S. Rafferty, G.H. Gilmer, M. Jaraíz, J.M. Poate, H.S. Luftman, T.E. Haynes, J. Appl. Phys. **81**, 6031 (1997)
8. N. Arai, S. Takeda, M. Kohyama, Phys. Rev. Lett. **78**, 4265 (1997)
9. M. Kohyama, S. Takeda, Phys. Rev. B **60**, 8075 (1999)
10. N.E.B. Cowern, G. Mannino, P.A. Stolk, F. Roozeboom, H.G.A. Huizing, J.G.M. van Berkum, F. Cristiano, A. Claverie, M. Jaraíz, Phys. Rev. Lett. **82**, 4460 (1999)
11. J. Kim, F. Kirchhoff, J.W. Wilkins, F.S. Khan, Phys. Rev. Lett. **84**, 503 (2000)
12. A. Bongiorno, L. Colombo, F. Cargnoni, C. Gatti, M. Rosati, Europhys. Lett. **50**, 608 (2000)
13. H. Jónsson, G. Mills, K.W. Jacobsen, in *Classical and Quantum Dynamics in Condensed Phase Simulations*, edited by B.J. Berne, G. Ciccotti, D.F. Coker (World Scientific, Singapore, 1998), p. 385
14. G. Henkelman, B.P. Uberuaga, H. Jónsson, J. Chem. Phys. **113**, 9901 (2000)
15. G. Henkelman, H. Jónsson, J. Chem. Phys. **111**, 7010 (1999)
16. T.J. Lenosky, J.D. Kress, I. Kwon, A.F. Voter, B. Edwards, D.F. Richards, S. Yang, J.B. Adams, Phys. Rev. B **55**, 1528 (1997)
17. S. Birner, J. Kim, D.A. Richie, J.W. Wilkins, A.F. Voter, T. Lenosky, Solid State Comm. **120**, 279 (2001)
18. S.K. Estreicher, M. Gharaibeh, P.A. Fedders, P. Ordejón, Phys. Rev. Lett. **86**, 1247 (2001)
19. G. Kresse, J. Hafner, Phys. Rev. B **47**, 558(R) (1993)
20. G. Kresse, J. Furthmüller, Phys. Rev. B **54**, 11169 (1996)
21. J.P. Perdew, in *Electronic Structure of Solids '91*, edited by P. Ziesche, H. Eschrig (Akademie Verlag, Berlin, 1991), p. 11
22. D. Vanderbilt, Phys. Rev. B **41**, 7892(R) (1990)
23. G. Kresse, J. Hafner, J. Phys.: Condens. Matter **6**, 8245 (1994)
24. D.A. Richie, J. Kim, S.A. Barr, K.R.A. Hazzard, R. Hennig, J.W. Wilkins, Phys. Rev. Lett. **92**, 045501 (2004)
25. G.H. Vineyard, J. Phys. Chem. Solids **3**, 121 (1957)
26. Y.A. Du, S.A. Barr, K.R.A. Hazzard, T.J. Lenosky, R.G. Hennig, J.W. Wilkins, Phys. Rev. B **72**, 241306(R) (2005)
27. Y.A. Du, R.G. Hennig, J.W. Wilkins, Phys. Rev. B **73**, 245203 (2006)
28. We ignore the saddle points which have TB formation energies of >3 eV with respect to the I_4-chain
29. In contrast, five of these eleven neighboring local minima have lower formation energies of 0.48, 0.51, 0.57, 0.78 and 0.84 eV above the I_4-chain. These five low-lying structures are distorted I_4-chains. The other six neighboring local minima, that have higher formation energies, are ignored here
30. P. Partyka, Y. Zhong, K. Nordlund, R.S. Averback, I.M. Robinson, P. Ehrhart, Phys. Rev. B **64**, 235207 (2001)
31. G.M. Lopez, V. Fiorentini, Phys. Rev. B **69**, 155206 (2004)
32. The total formation energy of an isolated I_3-chain and a single interstitial is about 2.1 eV above an I_4-chain.
33. P. Alippi, L. Colombo, Phys. Rev. B **62**, 1815 (2000)
34. We also relax the transition path shown in Figure 5 within TB model and obtain a barrier of 0.7 eV for a system to transform from an I_4-chain to a ground state I_4^a.
35. Two hundred dimer searches do not find any lower barrier.
36. J. Kim, F. Kirchhoff, W.G. Aulbur, J.W. Wilkins, F.S. Khan, G. Kresse, Phys. Rev. Lett. **83**, 1990 (1999), Kim et al. proposed a di-interstitial structure, I_2^a, for the $P6$ center, I_2^a is believed to be the ground-state di-interstitial, and it is highly mobile structure with a diffusion barrier of 0.3 eV (see Ref. [27])